Signal reconstruction of the slow wave and spike potential from electrogastrogram [1]

Shujia Qin [a,b,*], Wei Ding, Lei Miao [a], Ning Xi [a,c], Hongyi Li [a] and Chunmin Yang [d]

[a] *State Key Laboratory of Robotics, Shenyang Institute of Automation, Chinese Academy of Sciences, Liaoning Province 110016, PRC*
[b] *University of Chinese Academy of Sciences, No. 19A Yuquan Road, Beijing 100049, PRC*
[c] *Department of Electrical and Computer Engineering, Michigan State University, East Lansing, Michigan 48824, USA*
[d] *GI Department of Air Force General Hospital, Beijing 100142, PRC*

Abstract. The gastric slow wave and the spike potential can correspondingly represent the rhythm and the intensity of stomach motility. Because of the filtering effect of biological tissue, electrogastrogram (EGG) cannot measure the spike potential on the abdominal surface in the time domain. Thus, currently the parameters of EGG adopted by clinical applications are only the characteristics of the slow wave, such as the dominant frequency, the dominant power and the instability coefficients. The limitation of excluding the spike potential analyses hinders EGG from being a diagnosis to comprehensively reveal the motility status of the stomach. To overcome this defect, this paper a) presents an EGG reconstruction method utilizing the specified signal components decomposed by the discrete wavelet packet transform, and b) obtains a frequency band for the human gastric spike potential through fasting and postprandial cutaneous EGG experiments for twenty-five human volunteers. The results indicate the lower bound of the human gastric spike potential frequency is 0.96±0.20 Hz (58±12 cpm), and the upper bound is 1.17±0.23 Hz (70±14 cpm), both of which have not been reported before to the best of our knowledge. As an auxiliary validation of the proposed method, synchronous serosa-surface EGG acquisitions are carried out for two dogs. The frequency band results for the gastric spike potential of the two dogs are respectively 0.83–0.90 Hz (50–54 cpm) and 1.05–1.32 Hz (63–79 cpm). They lie in the reference range 50–80 cpm proposed in previous literature, showing the feasibility of the reconstruction method in this paper.

Keywords: Electrogastrogram (EGG), gastric spike potential, discrete wavelet transforms, wavelet packets

1. Introduction

Electrogastrogram (EGG) is a non-invasive analysis for gastric myoelectrical activity (GMA) whose components include the slow wave and the spike potential. By applying a high input impedance amplifier to measure the voltage signal on the abdominal surface, EGG can obtain the gastric slow wave along

*Address for correspondence: Shujia Qin, State Key Laboratory of Robotics, Shenyang Institute of Automation, Chinese Academy of Sciences, Liaoning Province 110016, PRC. Tel.: +86 024 23970726; E-mail: qinshujia@sia.cn.

with noises such as electrocardiogram (ECG), respiratory artifact, motion artifact, electrical interference of small intestine, and the electrode-skin interface noise [1]. The parameters of the gastric slow wave, e.g., the dominant frequency, the dominant power, and the instability coefficients, have been widely investigated and introduced into clinical applications to show gastric myoelectric abnormalities in patients with unexplained nausea and vomiting or functional dyspepsia [2]; however, although the relationship between GMA and the gastric motility has been observed—the gastric slow wave and the spike potential can correspondingly represent the rhythm and the intensity of stomach motility [3–7]—EGG is still unable to clearly approximate to GMA and therefore has not been considered as a rigorous diagnosis [8,9]. Currently, the main limitation of the measurement and analysis technique of EGG is that the method excludes the characteristics of the spike potential contained in the cutaneous EGG. It hinders EGG from comprehensively revealing the motility status of the stomach. In order to remedy this defect, besides acquiring cleaner slow waves, methods of extracting the spike potential should be developed.

The slow wave originates from the interstitial cells of Cajal (ICC) near the cardia of the stomach. For humans, the pacemaker depolarizes with a regular frequency range 2.4–3.7 cycles per minute (cpm) [10–12], and for dogs the normal value is approximately 5 cpm [13–15]. Classic methods for picking up the slow wave from EGG are bandpass filters [16], phase-locking filters, and autoregressive modeling. Afterwards, advance processing techniques, such as adaptive filtering [17], empirical mode decomposition [18], and independent component analysis (ICA) [19], are also introduced. Current trend of research is utilizing a multichannel acquisition system to record synchronous multichannel signals for dereferencing the respiratory artifact or separating independent signal components.

The spike potential contained in GMA can be observed through serosal electromyogram (EMG) during gastric peristaltic contractions; however, both the simulation [20] and experiment [1] show that due to the filtering effect of abdominal tissue, cutaneous EGG can not pick up the waveform of spikes, but only the slow wave or the increasing power caused by spikes [3]. In clinical practice, postprandial EGG records are often compared with fasting ones by power spectral density to evaluate the effect of spike potential [21–23], and then the stomach motility is indirectly studied. This comparison is considered to be inaccurate, because the spectral increment occurs over the whole frequency domain without distinguishing the component of spike potential.

In order to present both the slow wave and spike potential of the cutaneous EGG in the time domain and highlight the characteristics of the latter one, this paper proposes an EGG reconstruction method utilizing the specified signal components decomposed by the discrete wavelet packet transform, and obtains the normal frequency bands of the human gastric spike potential through fasting and postprandial cutaneous EGG experiments for twenty-five human volunteers. As an auxiliary validation, synchronous serosa-surface EGG acquisitions are carried out for two dogs.

2. Experimental protocol

2.1. The data acquisition system

The data acquisition system consists of a precise voltage amplifier and a data acquisition card: the four-channel low-drift differential amplifier with a 20 Hz low-pass filter at -3 dB in log magnitude, and the National Instrument™ USB-6229 BNC data acquisition (DAQ) card. The amplification factor of the amplifier is calibrated by the Tektronix™ AFG3102 dual channel arbitrary/function generator and set to about 200. The DAQ card is set to an input range of ±5 V with sampling rates of 100 Hz (for experiments

of dogs and human Group No. 1) and 14 Hz (for experiments of human Group No. 2). Because of a 16-bit resolution of the DAQ card, this input range corresponds to about 0.15 mV and will be suitable for the EGG acquisition.

2.2. Data acquisition for volunteers

Informed consents were obtained from all subjects prior to their participations. None of the subjects had evidence or known history gastrointestinal disorders. This project was approved by the Ethics Committee of Air Force General Hospital. Two volunteer groups were included in this study—Group No. 1: fifteen adult volunteers (ten males and five females) of age 26.3±3.2 years, weight 53.1±7.9 kg, and height 169.5±5.5 cm in the *mean±standard deviation* notation. These experiments were conducted in Shenyang Institute of Automation, Chinese Academy of Sciences, Shenyang, China. Group No. 2: ten adult volunteers (seven males and three females) of age 30.2±3.1 years, weight 62.7±13.4 kg, and height 171.1±7.7 cm. These experiments were conducted in Shengjing Hospital of China Medical University, Shenyang, China.

The data acquisition was conducted following the steps: 1) Four-channel Ambu™ type-Q Blue electrodes with the same reference were placed on the abdomen skin around the stomach in accordance with the scenario proposed by [21]: the third electrode was fixed in the middle between the xiphoid process and the umbilicus; the fourth electrode was horizontally attached 4–6 cm to the left of the third electrode; the second and the first electrodes were placed with an interval of 4–6 cm on the upper right side of the third one. Ensure the impedance was less than 30 kΩ. Fasting cutaneous EGG data was recorded for twenty minutes. The channel with the best signal-noise ratio in each record was used in the data processing. 2) Keeping the sensors being pasted on the skin, a meal stimuli was carried out within a given block: 300 mL water, 150 g rice (174 kcal), an egg (72 kcal), 200 g cabbages (44 kcal), and 200 g beef (212 kcal). For convenience, the experiment was conducted around the lunch time. 3) After the meal, postprandial cutaneous EGG data was recorded for one hour. Similar to the fasting case, the channel with the best signal-noise ratio in each record was used in the data processing.

2.3. Data acquisition for dogs

Two Kunming dogs weighing 17.2 kg and 23.6 kg were treated in accordance with the Animal Experimental Guides of Air Force General Hospital. This project was also approved by the Ethics Committee of Air Force General Hospital. The experiments followed the steps: 1) A pair of Ambu™ type-Q Blue sensors were placed on the abdomen near the gastric antrum after the skin shaving treatment. If the impedance between the two sensors was larger than 30 kΩ, the skin would be further polished with a piece of abrasive paper until the impedance meets the requirement, and then the sensors were replaced by new ones. When the sensors worked well, cutaneous EGG data were recorded for twenty minutes. 2) The ketamine hydrochloride was diluted into concentration of 10 mg/ml and used for intravenous anaesthesia at a dosage of 1 ml/kg. After the anaesthesia treatment, a pair of stainless steel electrodes were planted on the gastric antrum serosa by suturing. Wires were connected to the electrodes, then well isolated, and led to the amplifier outside the body. 3) Cutaneous EGG and in vivo serosal electromyogram were recorded synchronously for twenty minutes. 4) In order to stimulate the stomach to contract, intravenous injection of erythromycin was performed at a dosage of 2 mg/kg. After spike potential could be seen in the serosal electromyogram, cutaneous and serosal data were recorded synchronously for twenty minutes. 5) All the experimental data were measured under anaesthesia. After finishing the recording, all the electrodes and the wires were removed, and the wounds were treated by suturing.

2.4. Experiment design

Because the cutaneous EGG cannot directly measure the waveform of spikes, an indirect experiment design should be made to demonstrate the reconstruction result actually presents the spike potential. Thus, the procedure in this paper is designed following this logic flow: 1) Synchronous serosa-surface EGGs are measured from dogs. As the spikes in the serosal record can be recognized to be the actual spike potential in the time domain [7], the spike reconstruction data of the corresponding simultaneous surface record via the proposed method can be confirmed as the spike potential if it is similar to that in the serosal record. 2) The biomedical characteristics of the stomach between humans and dogs are analogous, e.g. the dominant frequencies of the slow wave are respectively 2.4–3.7 cpm for humans [10] and about 5 cpm for dogs [13], the volumes are respectively 2–4 L for humans [24] and about 2.5 L for dogs [25]. 3) Cutaneous EGGs are measured from human volunteers. If through the proposed reconstruction method, distinctions between fasting and postprandial EGG records from the same human subject can be observed, and the pattern of extracted spikes is similar to that in the canine case, then these will indicate that the spike reconstruction result from the human cutaneous EGG *very likely* presents the spike potential. The sections below will demonstrate the feasibility of the proposed method for the human spike detection via abdominal surface in this way.

3. Methods

3.1. The wavelet packet decomposition and reconstruction with band selection

The wavelet transforms measure similarity between a signal and a wavelet function by using inner products. The approximation of a signal f at a resolution 2^{-j} can be defined as an orthogonal projection P. Besides the approximation spaces $\mathbf{V}_j \in L^2(\mathbb{R})$, if we also divide the detail spaces $\mathbf{W}_j$ by an orthonormal basis, we can obtain a binary wavelet packet tree. Let $\mathbf{W}_j^k$ be the kth detail space at the scale 2^j in the full binary wavelet packet tree, a signal f can be reconstructed by $f = \sum_{k=0}^{2^j-1} P_{\mathbf{W}_j^k} f$ at any scale 2^j [26]. According to the Nyquist-Shannon sampling theorem, after sampling by $x[n] = f(n/F_s)$, $n \in \mathbb{Z}$, the discretized signal x has a limit band of $[0, F_s/2)$ for reconstructable components. Similarly, such band for $P_{\mathbf{W}_j^k} f$ will be $B_j^k \triangleq [F_s k/2^{j+1}, \ F_s(k+1)/2^{j+1})$, and thus at the jth level the frequency domain resolution is $F_s/2^{j+1}$. We can estimate the energy of a signal component with the frequency range B_j^k and then obtain an energy spectrum by $\hat{P}(B_j^k) = \|P_{\mathbf{W}_j^k} f\|^2$. Setting a proper fixed j, for most narrow-band signals, only a few spaces $\mathbf{W}_j^k$ corresponding to the frequency domain are significant. Therefore, similar to a frequency-domain filter, the recovered signal $\tilde{f}_\Gamma$ with the selected band set $\Gamma \subseteq \{0, 1, \ldots, 2^j - 1\}$ can be calculated by $\tilde{f}_\Gamma = \sum_{k \in \Gamma} P_{\mathbf{W}_j^k} f$.

3.2. Criteria for frequency band of the spike potential

During the occurrence of the gastric peristaltic contraction, energy increment of EGG can be observed in a wide frequency band [5]. Outstandingly, the band of spike potential will have more energy than adjacent bands due to the presence of spike potential activity [7]. Thus, to compare the postprandial data with the fasting data, and conclude the frequency band of the spike potential, criteria via the energy increment are defined as: 1) Set a fixed observation frequency $[0.5, 2.0]$ Hz (for humans) or $[0.7, 2.0]$ Hz
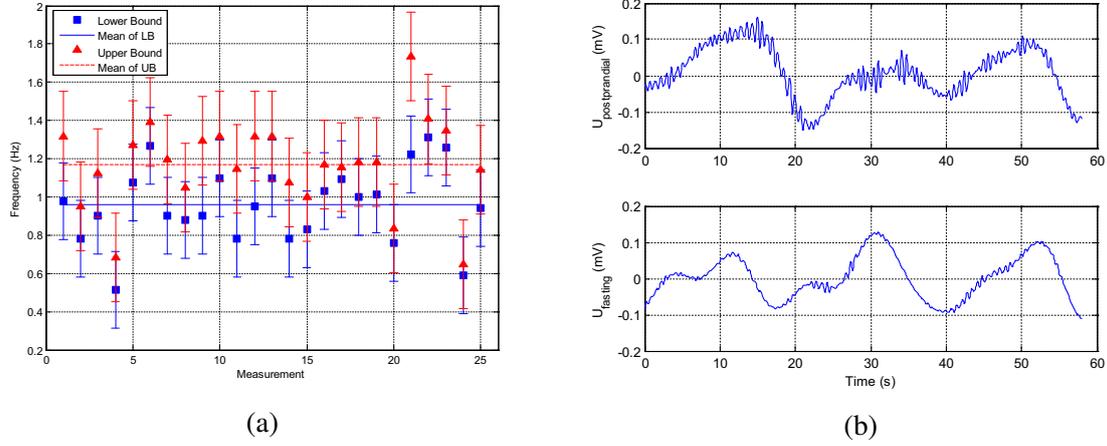
Fig. 1. EGG reconstructions for human volunteers: (a) Frequency bands of the human gastric spike potential in twenty-five experiments. Error bars represent the standard deviation of uncertainty for lower bounds (LBs) or upper bounds (UBs). (b) the comparison of reconstructed cutaneous EGGs in fasting status (bottom) and postprandial status (top).

(for dogs). 2) Calculate the average of energy increment in this band as a reference line. 3) Mark the largest continuous interval where the spectrum is above the reference line. This interval is then considered as the frequency band for the spike potential.

3.3. Procedure of data processing

Each record of the experimental data is processed following these steps: 1) Calculate the energy spectrum of the record using $\hat{P}(B_j^k) = \|P_{\mathbf{W}_j^k} f\|^2$. The Daubechies-9 (DB9) wavelet base is selected for decomposition and reconstruction. In consideration of the typical frequencies of slow wave spike for humans (0.05 Hz) and for dogs (0.08 Hz), the decomposition level is set to be eleven so that the resolutions of the frequency domain are respectively 0.024 Hz for sampling rate 100 Hz and 0.0034 Hz for sampling rate 14 Hz. 2) Determine the frequency band of the spike potential according to the criteria stated in Section 3.2.

Specially, for the frequency band results of human records, analyses of mean and standard deviation are carried out to conclude empirical frequency bounds of the human gastric spike potential. By using the achieved spike band along with the slow wave frequency band $[0.03, 0.08]$ Hz, the human EGG signals are recovered.

4. Results

The total twenty-five volunteer records are processed using the proposed procedure. Results are shown in Figure 1(a). The twenty-five spike band results conclude that the lower bound of the human gastric spike potential frequency is 0.96±0.20 Hz (58±12 cpm) and the upper bound is 1.17±0.23 Hz (70±14 cpm). Thus, the human EGG reconstructions are proposed to recover the frequency bands $[0.03, 0.08]$ Hz (1.8–4.8 cpm) and $[0.96, 1.17]$ Hz (58–70 cpm). A comparison of reconstructed cutaneous EGGs in fasting status and postprandial status, whose amplitude of the spike component can be clearly distinguished, is shown in Figure 1(b).
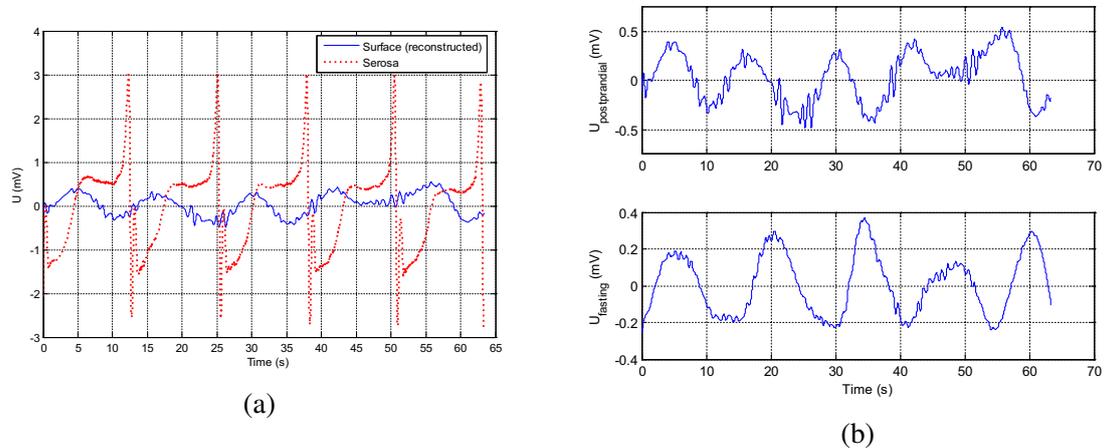
Fig. 2. EGG reconstructions for dogs: (a) the comparison of reconstructed cutaneous EGG and synchronous serosal EGG; (b) the comparison of reconstructed cutaneous EGGs in fasting status (bottom) and postprandial status (top).

The auxiliary evidence of the feasibility of the proposed method, i.e. the result of the canine experiments, is shown in Figure 2. Detected by the proposed criteria, the gastric spike bands for the two dogs are respectively 0.83–0.90 Hz (50–54 cpm) and 1.05–1.32 Hz (63–79 cpm). Both bands of canine gastric spike potential lie in the reference range 50–80 cpm proposed in [7, 27]. Figure 2(a) shows the synchronous serosal EGG and the reconstructed cutaneous EGG; because the phases of GMA signals from the stomach fundus and body lead ahead of that from the stomach antrum, the surface data mixing all EGG signals with different phases appear more advance than the serosal data. Figure 2(b) shows the comparison of reconstructed cutaneous EGGs in fasting status and postprandial status; this result is similar to the human EGG reconstructions shown in Figure 1(b).

5. Conclusion

This paper aims to develop a method that can present the spike potential of the cutaneous EGG as well as the slow wave in the time domain. The discrete wavelet packet transform is utilized to decompose the experimental measurement data and extract the desired frequency bands of the human gastric spike potential. Synchronous serosa-surface EGG acquisitions from dogs serve as the auxiliary validation of our method. Results indicate that the reconstruction is able to differentiate the fasting and the postprandial EGG signals in the time domain, and referencing the canine experiments, the frequency band detection method is feasible for humans.

References

[1] J. Chen and R. W. McCallum, Clinical applications of electrogastrography, The American Journal of Gastroenterology **88** (1993), 1324–1336.

[2] Henry P. Parkman, William L. Hasler and Robert S. Fisher, American gastroenterological association technical review on the diagnosis and treatment of gastroparesis, Gastroenterology **127** (2004), 1592–1622.

[3] A. J. P. M. Smout, J. van der Schee and L. L. Grashuis, What is measured in electrogastrography, Digestive Diseases and Sciences **25** (1980), 179–187.

[4] C. Y. You and W. Y. Chey, Study of electromechanical activity of the stomach in humans and in dogs with particular attention to tachygastria, Gastroenterology **86** (1984), 1460–1478.

[5] K. L. Koch and R. M. Stern, Electrogastrographic data acquisition and analysis: The penn state experience, Electrogastrography: Principles and Applications J. Z. Chen and R. W. McCallum, eds., Raven, New York, 1994, pp. 31–44.

[6] M. Tokmakci, Analysis of the electrogastrogram using discrete wavelet transform and statistical methods to detect gastric dysrhythmia, Journal of Medical Systems **31** (2007), 295–302.

[7] A. Akin and H. H. Sun, Time-frequency methods for detecting spike activity of stomach, Medical & Biological Engineering & Computing **37** (1999), 381–390.

[8] D. A. Drossman, E. Corazziari, M. Delvaux, R. C. Spiller, N. J. Talley, W. G. Thompson and W. E. Whitehead, Rome III: The Functional Gastrointestinal Disorders, 3rd ed., Degnon Associates Inc., McLean, VA, 2006.

[9] HP Parkman, WL Hasler, JL Barnett and EY Eaker, Electrogastrography: a document prepared by the gastric section of the american motility society clinical gi motility testing task force, Neurogastroenterology & Motility **15** (2003), 89–102.

[10] M. A. M. T. Verhagen, Electrogastrography, Clinical Autonomic Research **15** (2005), 364–367.

[11] Ronald A Hinder and Keith A Kelly, Human gastric pacesetter potential: site of origin, spread, and response to gastric transection and proximal gastric vagotomy, The American Journal of Surgery **133** (1977), 29–33.

[12] Gregory O'Grady, Peng Du, Leo K Cheng, John U Egbuji, Wim JEP Lammers, John A Windsor and Andrew J Pullan, Origin and propagation of human gastric slow-wave activity defined by high-resolution mapping, American Journal of Physiology-Gastrointestinal and Liver Physiology **299** (2010), G585–G592.

[13] A. C. W. Volkers, E. J. van der Schee and J. L. Grashuis, Electrogastrography in the dog: waveform analysis by a coherent averaging technique, Medical & Biological Engineering & Computing **21** (1983), 56–64.

[14] KA Kelly, CHARLES F Code and LILA R Elveback, Patterns of canine gastric electrical activity, American Journal of Physiology–Legacy Content **217** (1969), 461–470.

[15] Wim JEP Lammers, Luc Ver Donck, Betty Stephen, Dirk Smets and Jan AJ Schuurkes, Origin and propagation of the slow wave in the canine stomach: the outlines of a gastric conduction system, American Journal of Physiology-Gastrointestinal and Liver Physiology **296** (2009), G1200–G1210.

[16] Niranchan Paskaranandavadivel, Gregory O'Grady, Peng Du, and L K Cheng, Comparison of filtering methods for extra-cellular gastric slow wave recordings, Neurogastroenterology & Motility **25** (2013), 79–83.

[17] Jian Chen and Zhiyue Lin, Comparison of adaptive filtering in time-, transform- and frequency-domain: An electrogastrographic study, Annals of Biomedical Engineering **22** (1994), 423–431.

[18] H. Liang, Z. Lin and R. McCallum, Artifact reduction in electrogastrogram based on empirical mode decomposition method, Medical and Biological Engineering and Computing **38** (2000), 35–41.

[19] C. Peng, X. Qian and D. Ye, Electrogastrogram extraction using independent component analysis with references, Neural Computing and Applications **16** (2007), 581–587.

[20] L. A. Bradshaw, W. O. Richards and J. P. Wikswo Jr, Volume conductor effects on the spatial resolution of magnetic fields and electric potentials from gastrointestinal electrical activity, Medical & Biological Engineering & Computing **39** (2001), 35–43.

[21] B. Krusiec-Swidergol and K. Jonderko, Multichannel electrogastrography under a magnifying glass – an in-depth study on reproducibility of fed state electrogastrograms, Neurogastroenterology & Motility **20** (2008), 625–634.

[22] J. R. Filho, J. M. de Rezende and J. R. D. C. Melo, Electrogastrography in patients with chagas' disease, Digestive Diseases and Sciences **50** (2005), 1882–1888.

[23] C. L. Chen, H. H. Lin, L. C. Huang, S. C. Huang and T. T. Liu, Electrogastrography differentiates reflux disease with or without dyspeptic symptoms, Digestive Diseases and Sciences **49** (2004), 715–719.

[24] H. Curtis and S.N. Barnes, Invitation to Biology, WORTH PUBL Incorporated, 1994.

[25] Henry C. Lin, Xiao-Tuan Zhao, Benjamin Chung, Y. G. Gu and Janet D. Elashoff, Frequency of gastric pacesetter potential depends on volume and site of distension, American Journal of Physiology-Gastrointestinal and Liver Physiology **270** (1996), G470–G475.

[26] Stéphane Mallat, A Wavelet Tour of Signal Processing: The Sparse Way, 3rd ed., Elsevier (Singapore) Pte Ltd., 2009.

[27] Ata Akin and Hun H Sun, Non-invasive gastric motility monitor: fast electrogastrogram (fegg), Physiological Measurement **23** (2002), 505.